

# On the Background Rate in the LXeGRIT Instrument during the 2000 Balloon Flight

A. Curioni<sup>a</sup>, E. Aprile<sup>a</sup>, K.L. Giboni<sup>a</sup>, M. Kobayashi<sup>a</sup>,  
U.G. Oberlack<sup>b</sup>, E.L. Chupp<sup>c</sup>, P.P. Dunphy<sup>c</sup>, T. Doke<sup>d</sup>, J. Kikuchi<sup>d</sup>, S. Ventura<sup>e</sup>,

<sup>a</sup>Columbia Astrophysics Laboratory, Columbia University

<sup>b</sup>Rice University

<sup>c</sup>University of New Hampshire

<sup>d</sup>Waseda University, Japan

<sup>e</sup>INFN and Università di Padova, Italy

## ABSTRACT

LXeGRIT is the first prototype of a novel Compton telescope for MeV  $\gamma$ -ray astrophysics based on a Liquid Xenon Time Projection Chamber (LXeTPC), sensitive in the energy band of 0.15 – 10 MeV. In this homogeneous, 3D position sensitive detector,  $\gamma$ -rays with at least two interactions in the sensitive volume of 2800 cm<sup>3</sup>, are imaged as in a standard Compton telescope.  $\gamma$ -rays with a single interaction cannot be imaged and constitute a background which can be easily identified and rejected. Charged particles and localized  $\beta$ -particles background is also easily suppressed based on the TPC localization capability with millimeter resolution. A measurement of the total  $\gamma$ -ray background rate in near space conditions and the background rejection power of the LXeTPC was a primary goal of the LXeGRIT balloon flight program. We present here a preliminary analysis addressing this question, based on balloon flight data acquired during the Oct 4-5, 2000 LXeGRIT balloon flight from Ft. Sumner, NM. In this long duration (27 hr) balloon experiment, the LXeGRIT TPC was not surrounded by any  $\gamma$ -ray or charged particle shield. Single site events and charged particles were mostly rejected on-line at the first and second trigger level. The remaining count rate of single-site  $\gamma$ -ray events, at an average atmospheric depth of 3.2 g cm<sup>-2</sup>, is consistent with that expected from atmospheric and diffuse  $\gamma$ -ray background, taking into account the instrument mass model and response.

**Keywords:** gamma-rays, instrumentation, telescope, balloon missions, high energy astrophysics

## 1. LXeGRIT 2000 BALLOON FLIGHT

The Liquid Xenon Gamma Ray Imaging Telescope (LXeGRIT) uses a Liquid Xenon Time Projection Chamber (LXeTPC) to image MeV  $\gamma$ -rays from the energy deposits and 3D spatial coordinates, measured on an event-by-event basis. The instrument and results from laboratory and previous balloon flight experiments in 1997 and 1999 are discussed in various references<sup>1-5</sup>. Here we focus on an analysis of data acquired during the last LXeGRIT balloon flight, when the LXeTPC was used without any  $\gamma$ -ray or charged particle shield. The flight took place on Oct 4–5, 2000, from Ft. Sumner, NM and lasted 27 hours, including ascent. Fig. 1 shows the altitude of the balloon payload and the corresponding atmospheric depth, which varies between 5.7 and 3.2 g cm<sup>-2</sup>.

The zenith distance of known celestial  $\gamma$ -ray sources during flight is shown in Fig. 2. The Crab nebula, among them the brightest in  $\gamma$ -rays, was in the LXeGRIT field of view - which we define within an angular distance of 60° - for more than 8 hours, from 7:00 to 15:30 UT. The analysis presented in this paper is based on single-site events recorded over 5 hours, from 12:00 to 17:00 UT, on October 5, 2000. In this period LXeGRIT was at a stable altitude of  $\sim 39$  km or  $\sim 3.2$  g cm<sup>-2</sup> atmospheric depth.

The overall goal of this analysis is to understand the measured background count rate in the LXeTPC. In the 2000 flight configuration, the instrument was sensitive in the energy range from  $\sim 150$  keV to 10 MeV. The LXeTPC trigger rate, provided by the primary scintillation light signal, was  $\sim 600$  Hz (Fig. 3, top panel). This rate was nearly constant throughout

---

Further author information: (Send correspondence to: Alessandro Curioni)

Columbia Astrophysics Laboratory, Columbia University, New York, NY, USA

E-mail: curioni@astro.columbia.edu

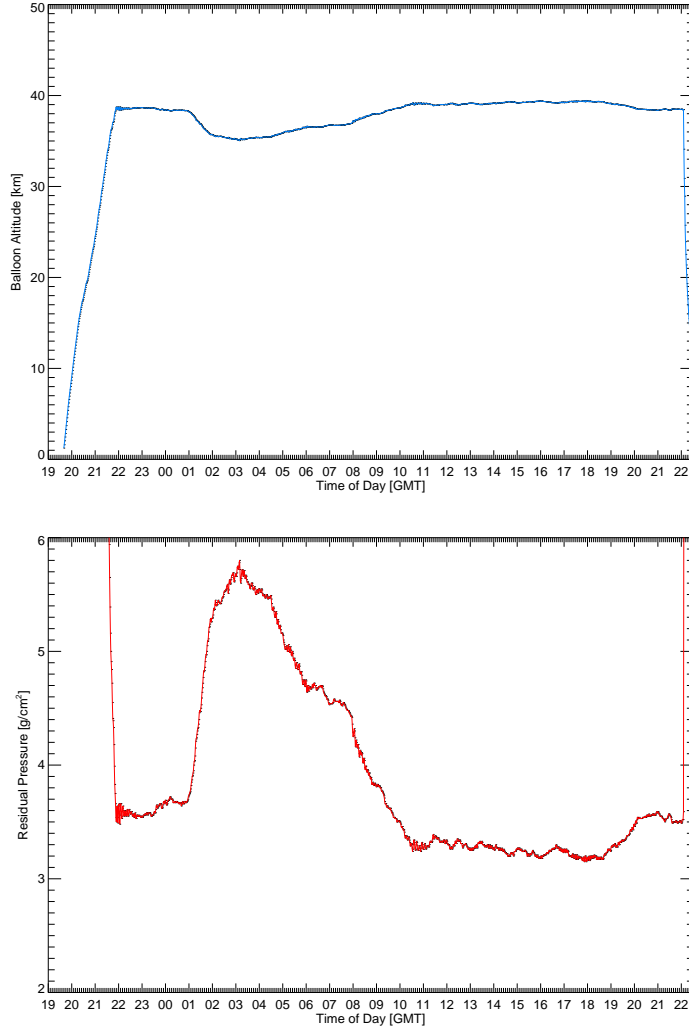


**Figure 1.** *Top:* Altitude of the balloon payload during the 2000 flight. *Bottom:* Atmospheric depth.

the flight, after ascent had been completed. The livetime fraction of the on-board data acquisition system (DAQ), shown in Fig. 3, bottom panel, was  $\sim 50\%$ . Since the LXeTPC itself has a deadtime of about  $50\ \mu\text{s}$  / event and for a rate of 600 Hz the deadtime fraction amounts to less than 5 %, the instrument deadtime is largely determined by the DAQ. The DAQ processor was able to handle  $\sim 300$  Hz (Built and Rejected Event rates are shown in Fig. 4) - the rejection rate at the second level trigger was  $\sim 250$  Hz, the rate of selected events  $\sim 50$  Hz, all of them transmitted to ground or written to the on-board hard disks. The “gaps” visible in the rate vs. time plots correspond to the TPC cooling periods during which the DAQ is turned off due to the increased noise level on the anodes, while the PMTs remain operational. More details about on-line event rejection are given in Sec. 1.1.

### 1.1. Event trigger and data acquisition

The LXeGRIT event trigger works on two different levels: the *first level trigger* requires a signal from at least one of the four PMTs detecting the light from the LXeTPC volume, while the *second level trigger* selects events based on the anodes / wires ionization signals recorded for each triggered event. Decisions at the second trigger level are made necessary by the limited DAQ speed (for a thorough and up-to-date account of the LXeGRIT DAQ see Aprile et al.<sup>6</sup>) which imposes an upper limit to the detector livetime, i.e. the maximum rate of events transmitted through telemetry or written to the

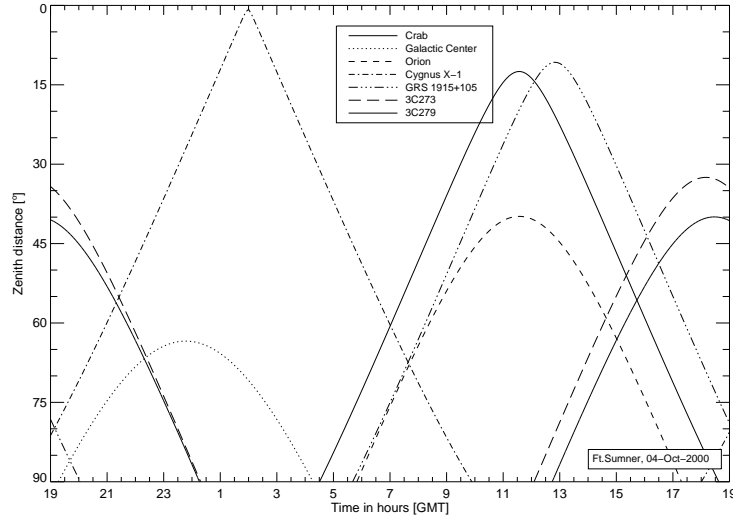


**Figure 2.** Known celestial  $\gamma$ -ray sources in the LXeGRIT field of view during the 2000 flight.

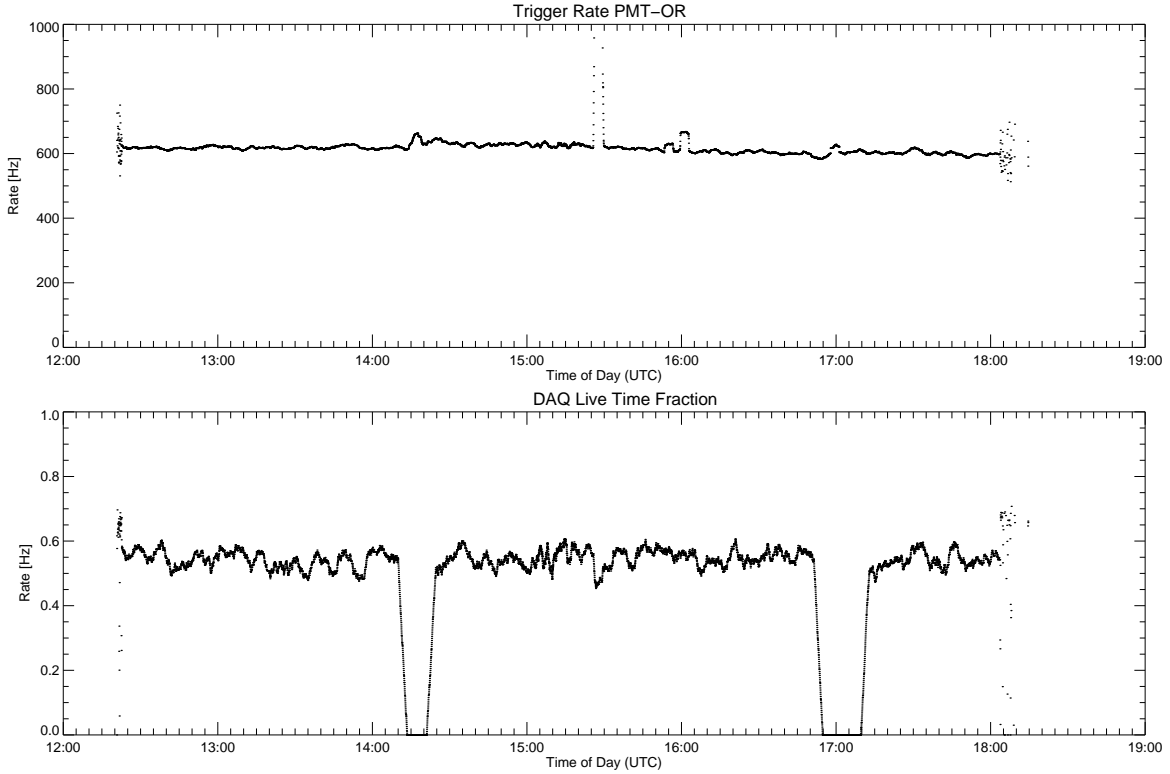


**Figure 3.** *Top:* PMT-OR rate, *bottom:* DAQ livetime fraction.

on-board disk (about  $150 \text{ evts sec}^{-1}$ , depending on the event size).

The *first level trigger* is provided by the OR of the four PMTs. This fast light signal starts the DAQ and marks the beginning of the drift time measurement. To avoid pile-up of independent events, it is required that there is no PMT signal within  $50 \mu\text{s}$  before the event. This trigger level allows a fast decision but it is rather insensitive to different event topologies or energies. Ideally a high trigger efficiency at this level would be desirable but in practice, given the soft energy spectrum

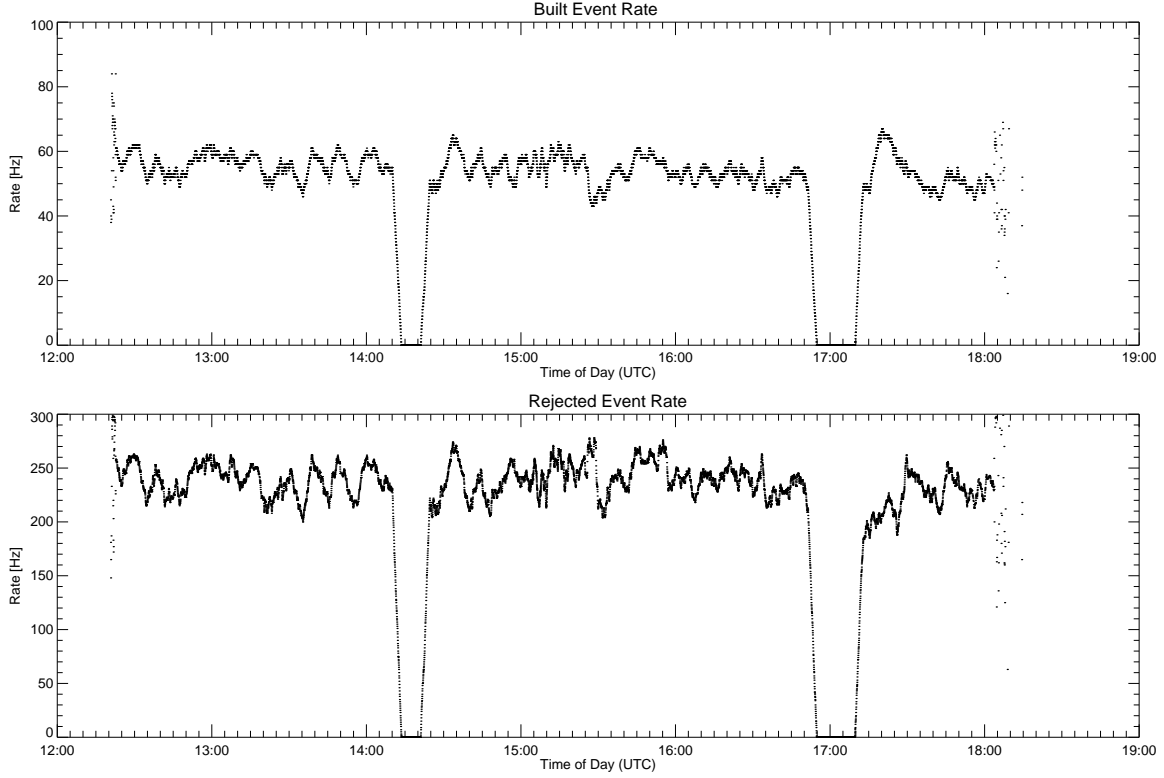


**Figure 4.** *Top:* selected event rate, *bottom:* rejected event rate.

of the atmospheric and cosmic diffuse  $\gamma$ -ray background this would be equivalent to accept a dominant fraction of low energy (150-500 keV) events which are of very little use for a Compton telescope like LXeGRIT with an energy threshold of  $\sim 150$  keV. The light trigger efficiency (LTE) for the 2000 flight has been measured for energies up to 2 MeV and spatially resolved with a few millimeter granularity. In flight configuration the LTE averaged over the active volume was 10-20 % in the energy range 1-2 MeV, steeply decreasing at lower energies. A similar measurement has been described in Oberlack et al.<sup>7</sup> for energies up to 500 keV and for the 1999 LXeGRIT settings of the light readout. The LTE is quite dependent on the location of the interaction inside the fiducial volume because of the varying solid angle viewed by the PMTs. Fig. 5 shows the solid angle effect on light collection by the z-dependence measured for one of the four PMT's, at an energy of 1.836 MeV. The strong dependence on interaction location requires a 3D spatial *times* 1D energy mapping of the efficiency,

The solid angle effect on light collection is shown by the z-dependence measured for one of the four PMTs (Fig. 5). The strong dependence on interaction location makes necessary a 4-D (x, y, z, energy) map of the light trigger efficiency, now fully implemented in the Monte Carlo simulation.

The *second level trigger* performs the following on-line selections: a. it requires a minimum and a maximum number of wire hits on each view (x and y) – with this MINMAX selection, the minimum rejects mostly single site events, the maximum rejects extended tracks due to high energy charged particle crossing the active volume; b. it requires a minimum signal amplitude above baseline on at least one anode - this requirement mainly rejects noise; c. it requires that the anode signal does not saturate the FADC, i.e. energy deposit on a single anode less than  $\sim 10$  MeV (flight 2000 settings) - this mainly rejects charged particles which deposit a large amount of energy in the active volume. Fig. 6 shows the impact of specific on-line selections on the flight data.

These on-line selections determine the type of event topologies accepted by LXeGRIT for further analysis. This option is relevant for a Compton telescope, since Compton imaging requires at least two interactions (Compton scattering followed by photoabsorption). In LXeGRIT, events with a single energy loss localized in one site of the sensitive volume (single site events) are easily recognized and rejected as background for source imaging. These events include either low energy  $\gamma$ -rays

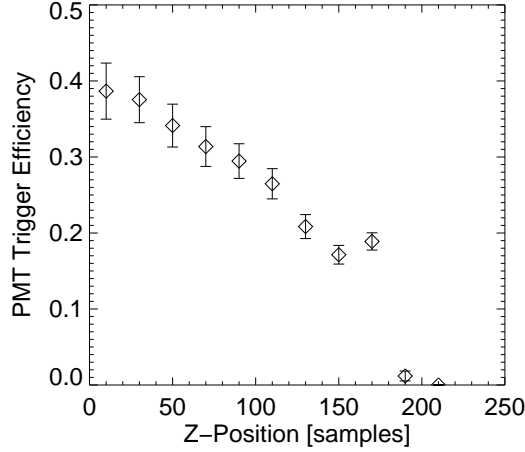


**Figure 5.** LTE vs.  $z$  position. The PMT is located below  $z=0$  and the solid angle effect is clearly visible.

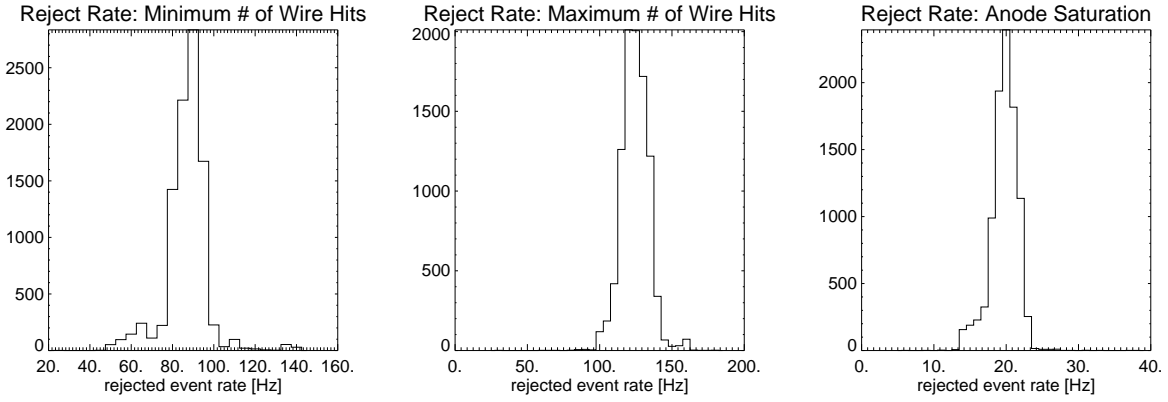


**Figure 6.** Distributions of rejected event rates due to specific selection at the second level trigger. *Left:* minimum number of wire hits both in  $x$  and  $y$ . *Center:* maximum number of wire hits in  $x$  or  $y$ . *Right:* anode saturation, i.e. an energy deposit larger than 10 MeV.

which are photoabsorbed or higher energy  $\gamma$ -rays which interact only once before escaping, as well as  $\alpha$ - or  $\beta$ -particles from internal background. The rejection power of the on-line MINMAX selection for single site events as a function of energy is shown in Fig. 7. It is better than 60 % for energies up to 4 MeV, i.e. for a large majority of the single site events (see Fig. 9). While effective, this second level trigger selection has the major drawback of taking DAQ time. Any remaining single site event can be rejected in the off-line analysis with efficiency very close to 100 %.

## 1.2. Off-line data reduction

A *raw event* consists of the digitized (62- $x$  and 62- $y$ ) wire and 4 anode signals, sampled at a frequency of 5 MHz. Going from the raw data to a data structure providing energy and 3D-position for each interaction, i.e.  $(x_1, y_1, z_1, E_1), \dots, (x_n, y_n, z_n, E_n)$ , where  $n$  is the interaction multiplicity, requires several steps of data processing.

In the first place, the analysis program identifies and rejects noisy events, events with interactions outside the fiducial volume, non- $\gamma$  events in general (e.g. charged particles).

A large fraction of the flight data are rejected at this stage of the analysis; in the end, about 20 % of the events are selected. Selected events are sorted according to their interaction multiplicity - this classification comes quite natural for a Compton telescope like LXeGRIT, since at least two interactions are required for Compton imaging and at least three interactions are required to determine the unique time sequence of the event. Since the Compton imaging capability of LXeGRIT is not exploited in the measurement presented here, we omit a discussion of the various issues pertaining to LXeGRIT as a Compton telescope, for which we refer to Oberlack et al..<sup>8</sup>

Having  $(x_i, y_i, z_i)$  for each interaction, fiducial volume selections can be applied. This kind of selection is very powerful

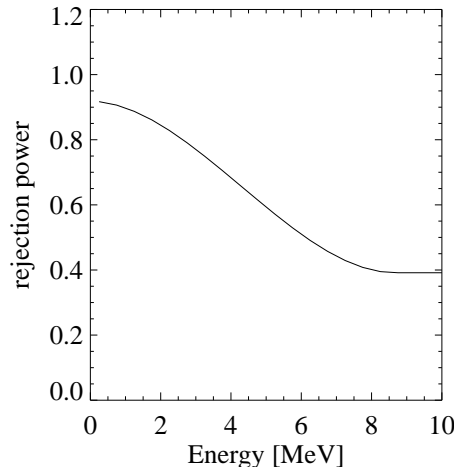


**Figure 7.** Rejection power of the MINMAX criterion for single site events.

(rejection power  $\sim 1$ ) in rejecting charged particle entering the TPC and localized (non- $\gamma$ ) internal background (see Sec. 2 and Sec. 4). A full imaging detector provides in fact a unique signature for charged particles. Since they lose energy continuously ionizing the active medium, the point where they enter the active volume is easily identified. The fine granularity allows a modest loss in fiducial volume. In this analysis, events with at least one interaction on the two outer wires (x or y coordinate - two wires correspond to 6 mm) or in the highest or lowest 3 mm along the z coordinate are rejected. After selections the fiducial volume is reduced to  $18.8 \times 18.8 \times 6.4 \text{ cm}^3$  (88 % of the original fiducial volume). The measured rates at the end of the off-line data reduction process, without correction for the detector livetime, are shown in Fig. 8, both for single and multiple interaction events. The count rate for single interaction events is  $\sim 0.7 \text{ Hz}$  while for multiple interaction events the rate is  $\sim 5 \text{ Hz}$ .

## 2. LXEGRIT IN-FLIGHT ENERGY SPECTRUM

The energy spectrum of single site events recorded at balloon altitude in the period 12:00 - 17:00 UT is shown in Fig. 9, left panel. It is largely dominated by low energy events, as expected (see Sec. 3 and Sec. 4). The lower energy threshold is  $\sim 150 \text{ keV}$ , given by the combined anode / wire signal-to-noise ratio. The high energy component is due to single-scatter Compton events and to pair production events in which the two 511 keV photons from positron annihilation both escape. The energy spectrum for multiple interaction events is also shown in Fig. 9, right panel. Compared to single site events, the spectrum is harder and the lower energy threshold is higher ( $\sim 300 \text{ keV}$ ), for at least two interactions must be above threshold. The clearly visible, especially in the multi-site events,  $^{40}\text{K}$  line is attributed to natural radioactivity of the ceramic (MACOR, which contains about 10 % potassium) used around the wire structure and field shaping rings. The small amount of  $^{40}\text{K}$  (we estimated  $\sim 10^{19}$  atoms of  $^{40}\text{K}$ ) and the clearness of the 1.465 MeV line, with the expected resolution, indicate the sensitivity of the detector. The  $^{40}\text{K}$  line turned out to be a very useful in-flight calibration tool. The internal instrumental background, especially its low energy (below 500 keV)  $\gamma$ -ray component, constitutes a sizeable fraction of the measured count rate. Repeated measurements in the laboratory have established the typical background spectrum in the LXeTPC on the ground, and allowed us to identify internal background sources. Subtraction of these contributions from the total background at balloon altitude is straightforward. The  $\gamma$ -ray background as measured at ground level, with the payload on the launch pad a few hours before the 2000 flight, is also shown in Fig. 9. The single site and multiple site energy spectra are shown separately. The multiple site spectrum shows more clearly the  $^{40}\text{K}$  line at 1.465 MeV while the single site spectrum is largely dominated by a component below 500 keV. Due to the more complex assessment of the strongly suppressed low-energy part of the single-site spectrum, we have not yet established how much of the low energy continuum is due to internal background and how much is due to local (environmental)  $\gamma$ -rays. The distinction is important since the one due to ambient activity does not contribute to the background at balloon altitude. In any case, this continuum is rather unimportant above several hundred keV.

In the study presented here the detector has been used as a spectrometer and single site events are as useful as multiple site events. A localized internal background source can be easily eliminated applying a fiducial volume cut. This is the

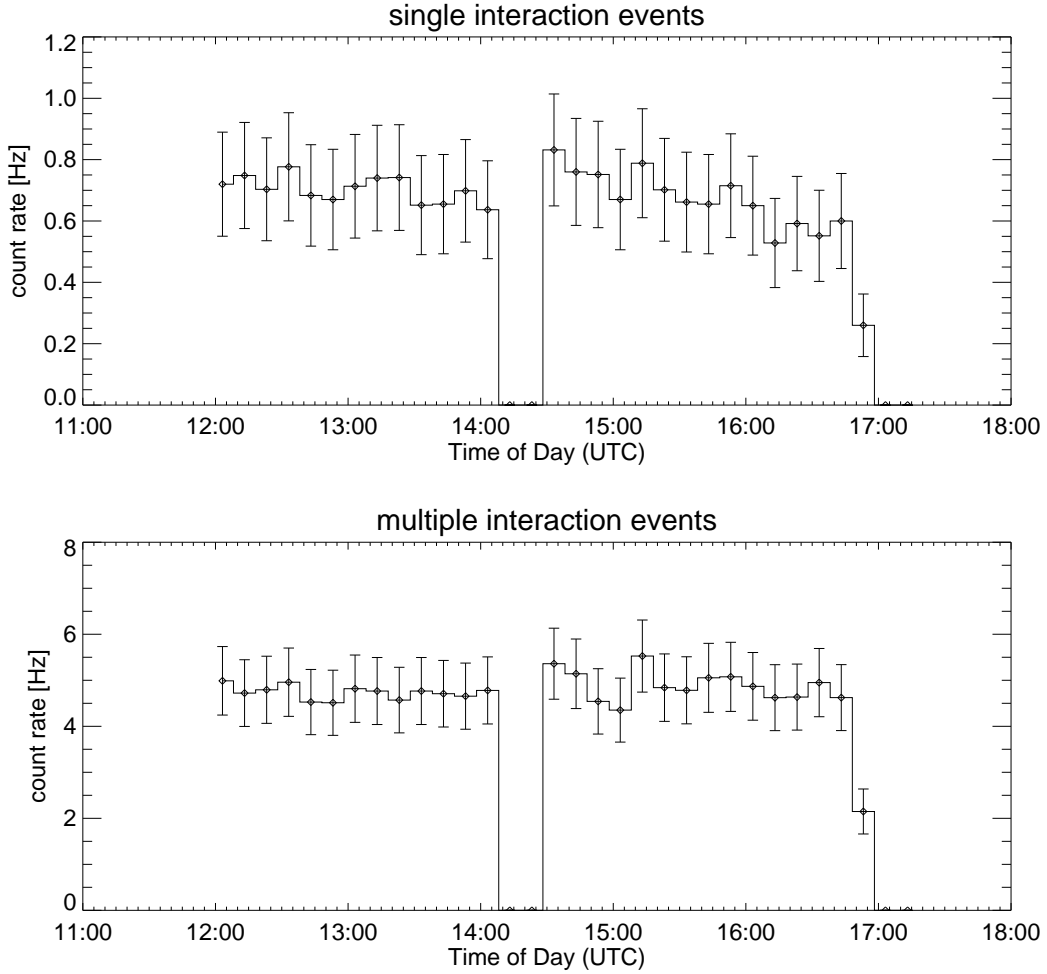


**Figure 8.** *Top:* measured rate for single interaction events, *bottom:* for multiple interaction events.

case of the localized, low energy events with  $z$ -position near the cathode (top of the detector - see Fig. 10). These events are likely due to  $\alpha$ -emission from the alumina substrate of the cathode plate \*. The same sharp (few mm) feature in the  $z$ -distribution has been detected both at the ground level and in flight with comparable strength. The fine granularity offers a very selective way to reject this background in the final data sample.

### 3. MONTE CARLO SIMULATION

#### 3.1. Mass Model

We have studied the propagation of atmospheric and cosmic diffuse  $\gamma$ -rays through a detailed model of the LXeGRIT instrument with a Monte Carlo simulation based on GEANT 3.21. In the flight 2000 configuration, LXeGRIT was operated without active shield and is thus an omni-directional detector in principle. Moreover, in this study of single-site events, we use LXeGRIT as a mere spectrometer without imaging information. It is therefore important to include the bulk of passive materials of the entire instrument, including the gondola, in the mass model, since these materials constitute significant mass for  $\gamma$ -ray attenuation and scattering. The total mass of the LXeGRIT instrument in flight configuration is  $\sim 1000$  kg; the TPC itself, including the stainless steel cold vessel and cryostat, is about 190 kg, of which 21 kg is liquid xenon. The  $20 \times 20 \times 7$  cm<sup>3</sup> box shaped fiducial volume of the TPC is enclosed in a 10 liter cylindrical vessel, filled with 7 liters

\*In a LXe detector simultaneously measuring ionization and scintillation light like LXeGRIT does,  $\alpha$  emission is identified by the small charge / light yield ratio.

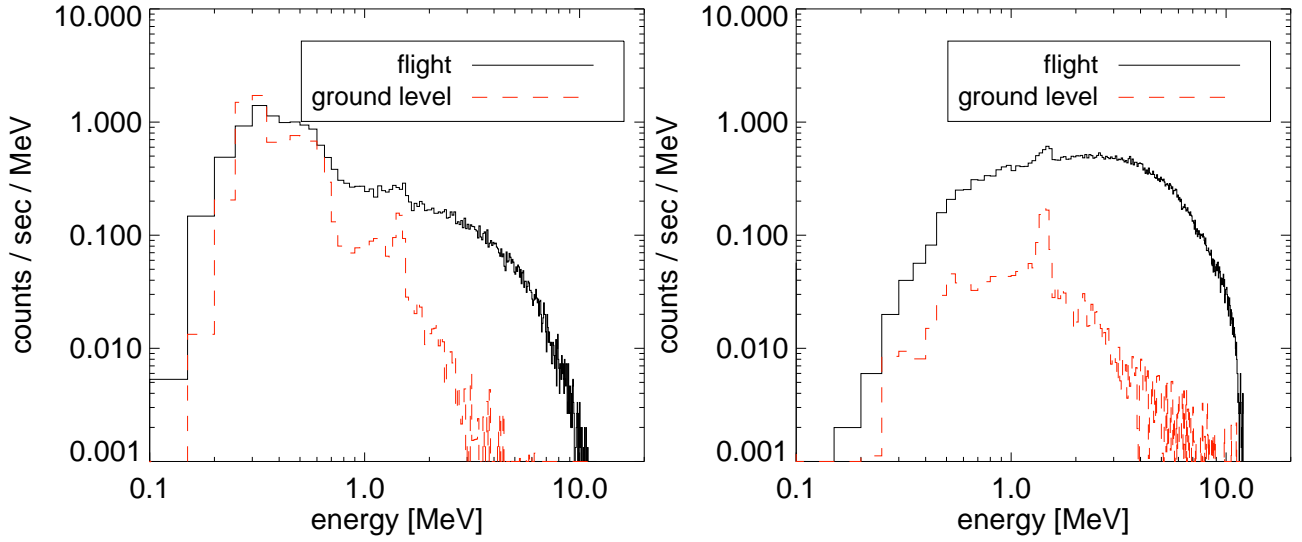


**Figure 9.** Energy spectra for flight data (*continuous line*) and for a background run at the ground level (*dashed line*). *Left:* single site events. *Right:* multiple interaction events.

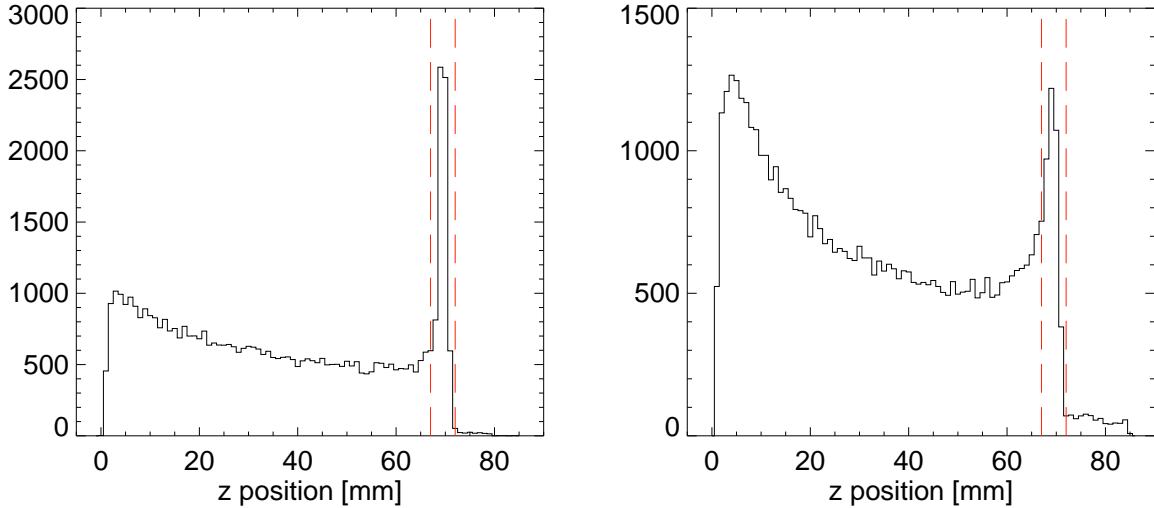


**Figure 10.** *Left:* Interaction depth (z coordinate) for single site events at the ground level. The top of the TPC (cathode) is located at  $z=70$  mm. *Right:* Interaction depth (z coordinate) for single site events during flight.

of pure liquid xenon. The remaining volume is filled with stainless steel blocks on three sides and a large ceramic HV feedthrough on the fourth side. The cold vessel is enclosed in a vacuum cryostat to provide thermal insulation. Both the vessel and the cryostat are made out of stainless steel and the walls are 3 mm thick for both vessels. The cryostat thickness is 7 mm on top and 20 mm on bottom; the vessel is 10 mm both on top and on bottom. On top of the TPC there is a “window”, i.e. both the cryostat and the vessel have been thinned (2 mm and 5 mm in the  $z$  direction, respectively) over a circle of diameter  $\sim 20$  cm. A layer of 5 mm of liquid xenon above the cathode and a layer of 3 cm below the anodes have also been taken into account. Passive materials below the TPC cryostat, i.e. the structure of the gondola, electronics boxes,  $\text{LN}_2$  dewar, battery stack etc. have been modeled as three aluminum plates of proper diameter and thickness located at different  $z$ -positions. The simulated instrument is 155 cm high ( $z$  direction) with a maximum diameter of 183 cm in the  $x$ - $y$  plane (diameter of the bottom aluminum plate).



### 3.2. Input Spectra

$\gamma$ -rays are started satisfying the spectral and geometrical properties of the specific source under study. For the case of interest in this paper, cosmic diffuse (CDG) and atmospheric (ATM)  $\gamma$ -rays were propagated through the LXeGRIT mass model. For the CDG we use the flux given by Schönfelder et al.<sup>11</sup>, i.e. an isotropic flux over the zenith angles from  $0^\circ$  to  $90^\circ$  following the power law  $0.011 E^{-2.3} \text{ cm}^{-2}\text{sec}^{-1}\text{sterad}^{-1}\text{MeV}^{-1}$ .<sup>†</sup> For the ATM, we follow the model given by Costa et al.,<sup>13</sup> for an atmospheric depth of  $3 \text{ g cm}^{-2}$ . The fluxes, in units of  $\text{cm}^{-2}\text{sec}^{-1}\text{MeV}^{-1}$ , are extrapolated in the energy range 100 keV - 15 MeV with four angular bins for the following zenith angles:

- $0.03 E^{-1.61} (0^\circ - 45^\circ)$
- $0.20 E^{-1.48} (45^\circ - 90^\circ)$
- $0.43 E^{-1.34} (90^\circ - 135^\circ)$
- $0.23 E^{-1.51} (135^\circ - 180^\circ)$

It is worthwhile stressing that the ATM flux is poorly known and suffers large uncertainties.

Each photon is propagated through the payload mass and, if the requirement of at least one interaction in the TPC fiducial volume is satisfied, energy deposit, location and interaction mechanism are recorded for each photon interaction. Photoabsorption is dominant at energies below 250 keV, while Compton scattering dominates up to  $\sim 6$  MeV, so that in this energy band  $\gamma$ -rays are mainly detected through multiple interactions. Above 6 MeV, pair production becomes increasingly important, together with secondary bremsstrahlung photons.

### 3.3. LXeGRIT Response Function to ATM+CDG

The task of the Monte Carlo program is to follow the propagation of the  $\gamma$ -rays through the various passive and active materials. For comparison with data, the detector response function has to be accurately modeled and applied to the physical interaction locations and energy deposits resulting from the basic MC simulation. Such factors include energy thresholds, various efficiencies, as well as realistic spatial and energy resolution. More specifically:

1. Light trigger efficiency: implemented on an event-by-event basis, using a look-up table as described in Sec. 1.1.
2. Efficiency of on-line selections at the second level trigger (MINMAX): the efficiency (or equivalently the rejection power) is routinely measured for each experiment and applied, accounting for its energy dependence (see Sec. 1.1).
3. A minimum energy threshold of 150 keV for detection of each interaction.
4. A minimum spatial separation of approximately of 5 mm on at least one coordinate between each pair of interactions in order to consider two interaction locations mutually resolved. If this condition is not fulfilled the two interactions are clustered and considered as one single interaction.
5. Energy resolution: 8.8 % (FWHM at 1 MeV) scaling as  $1/\sqrt{E}$  plus a noise term of 55 keV (FWHM) added in quadrature.
6. DAQ livetime fraction.
7. Efficiency of off-line selections.

Given the limited DAQ speed, the trigger efficiency during the 2000 flight was reduced for low energy events. The DAQ livetime fraction is easily and precisely accounted for, since it is measured by the DAQ processor itself. Given its complicated dependence on both position and energy, the light trigger efficiency is applied on an event-by-event basis (see Sec. 1.1). The MINMAX criterion has been parameterized as a function of energy only, assuming that (statistically) Monte Carlo events reproduce the topologies of real events (this is actually the case for calibration sources). In this way we do not test the criterion on each event but simply correct the energy spectrum with a function such as the one shown in Fig. 7.

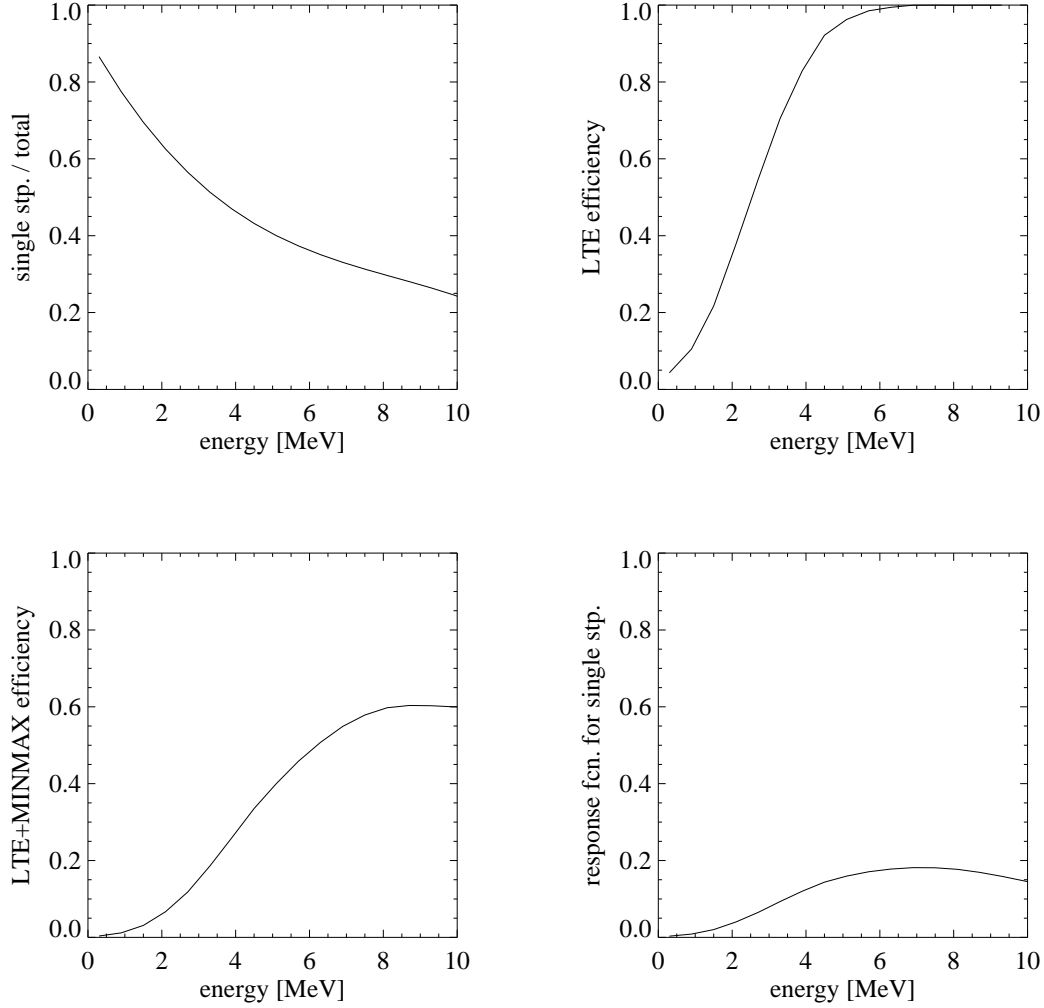


**Figure 11.** *Top left:* selecting single site events, *top right:* light trigger on single site events, *bottom left:* light trigger and MINMAX on single site events and, eventually, *bottom right:* single site selection, light trigger and MINMAX, i.e. the response function of LXeGRIT to ATM+CDG once the  $\gamma$ -rays have been transported through the instrument mass model. See text for more explanations.

Anode saturation is not considered in the simulation since it impacts only charged particles. Comparison of Monte Carlo data to calibration sources in the energy range 0.5 - 4.2 MeV has shown an excellent agreement.

For this paper we have not attempted to carefully model all multiplicities individually, but rather restrict ourselves to the case of single-site events. The more extensive work to properly account for all multiplicities is currently underway. Selecting single site events is part of the off-line selections and is well reproduced in the Monte Carlo simulation, at least in the energy range 0.5 - 4.2 MeV, where a comparison to calibration data is available. Fiducial volume selections are also easily accounted for in the simulation. Event quality selections (e.g. rejection of noisy events) are not considered in the present simulation. Several efficiencies entering the instrumental response function are summarized in Fig. 11. It is clear that, by design, the overall efficiency for single-site events is very low, with a steep energy dependence.

<sup>†</sup>More recent work has established the CDG flux to be 5–10 times smaller above 1 MeV, e.g. Kappadath et al.<sup>12</sup>. At these energies, however, the LXeGRIT background is fully dominated by atmospheric background in the current simulation already.

## 4. COMPARISON TO EXPECTATIONS

The expected background rate at balloon altitude can be split into two main parts: *a.* the total background rate, including charged particles, neutron induced background etc. and *b.* the ATM and CDG  $\gamma$ -ray background rate. The total background rate, with the 2000 flight settings, is basically given by the PMT-OR trigger rates in Sec. 1. To demonstrate the capability of LXeGRIT to measure cosmic  $\gamma$ -rays it is important to measure the ATM and CDG  $\gamma$ -ray contribution to the total background rate. A comparison to previous experiments and models is also relevant and is discussed in this section. We subdivide the total background in four categories:

1. charged particles
2. neutron induced background
3. instrumental background
4. ATM+CDG

### 4.1. Charged Particles (Primary and Secondary Cosmic Rays)

For a detector the size of LXeGRIT, the expected rate due to charged particles, both primary and secondary cosmic rays, is a few hundred Hz. A more precise estimate of the expected charged particle rate is beyond the scope of this paper and requires a model of primary and secondary cosmic ray fluxes to be propagated through the LXeGRIT mass model. Passive materials surrounding the TPC can attenuate charged particles up to hundred MeV, and cosmic rays may pass the sensitive volume only peripherally, depositing correspondingly low amounts of energy. In any case, we reject a large fraction of this component at the second level trigger. The MINMAX criterion provides a fairly high rejection power; events saturating the anode, i.e. energy deposits (order of) 10 MeV or larger are also rejected on-line. From a visual scan of data recorded without any selections applied at the second level trigger, we can infer that charge particles make about 2 / 3 of the total in-flight rate or about 400 Hz. Events not rejected on-line are rejected with an efficiency very close to one applying offline selections on the anode waveform and on the fiducial volume (see Sec. 1.2). To conclude, when measuring the  $\gamma$ -ray background, the contamination due to charged particles is reduced to a *truly negligible level*.

### 4.2. Neutrons

Due to its complexity, the neutron induced background would deserve a detailed and lengthy discussion on its own. A Monte Carlo simulation of the expected rate in LXeGRIT due to the atmospheric neutron flux, based on the GEANT3.21 / GCALOR<sup>10</sup> package and accounting for the induced  $\gamma$ -ray emission - to be described elsewhere in greater detail - indicate a marginal contribution to the overall rate.

From the data themselves, the lack of lines pointing to neutron activation indicates that the neutron induced background is of little importance in explaining the total background rate and, more specifically, the  $\gamma$ -ray background at balloon altitude. This finding is not surprising, given the well known radiation hardness of Xe compared to other scintillators or Ge, as found in laboratory measurements, i.e. monoenergetic irradiation at accelerator facilities, and in deep space (see Kirsanov et al.<sup>14</sup> and Ulin et al.<sup>15</sup>).

### 4.3. Instrumental Background

The instrumental background has been partially discussed in Sec. 2. The spallation local production background at balloon altitude is however not known. A preliminary calculation indicates that it is rather negligible compared to CDG and ATM fluxes, and we do not measure any appreciable excess in the count rate. A more detailed calculation is under way.

### 4.4. ATM+CDG

Using the Monte Carlo simulation described in Sec. 3 to transport the  $\gamma$ -rays and assuming an energy threshold of 150 keV, the expected ATM and CDG interaction rate in the XeTPC is  $\sim 100$  Hz. The atmospheric background is the dominant component, while the cosmic diffuse contributes  $\sim 10$  % of the total interaction rate at energies below 500 keV and becomes much less important at higher energies. Up to this point only the geometry and the mass model of the instrument are taken into account. These numbers are very far from the actual measured rate (see Sec. 1.2), since we do not yet include the instrument response function (Sec. 3.3). Therefore, in order to get to the final comparison we still have to correct the

Monte Carlo prediction with the detector response function, which is applied event-by-event (the one for the ATM+CGD is summarized in Sec. 3.3) The outcome of this analysis is shown in Fig. 12. The Monte Carlo expectation still overestimates the measured rate and an overall factor of 2 has been introduced to account for efficiency losses due to off-line rejection of noisy events and event quality selections.

The agreement is fairly good even if a certain discrepancy is present for energies lower than 1.5 MeV. This is mainly due to the fact that, at these energies, the intrinsic internal background, which is not included in the Monte Carlo simulation, plays some role (e.g. the prominent  $^{40}\text{K}$  line). The discrepancy is well within uncertainties in our model of the instrument and in the input fluxes.

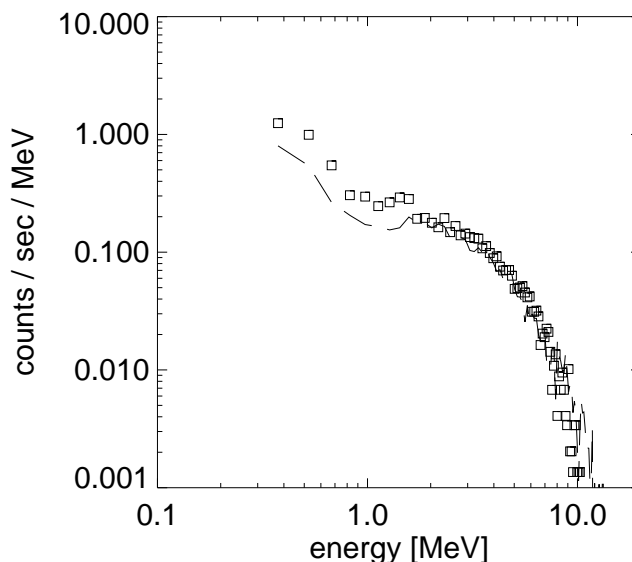


**Figure 12.** *Open squares* - Experimental data. *Dashed line* - Monte Carlo prediction. See text for explanation.

## 5. CONCLUSIONS

In this paper we have presented a measurement of the  $\gamma$ -ray background rate in the LXeGRIT Compton telescope from a sample of data acquired at  $3.2 \text{ g cm}^{-2}$  atmospheric depth during the 2000 balloon flight from Ft. Sumner, NM. The measured trigger rate at float altitude was about 600 Hz at the first level trigger. Of this about 400 Hz were charged particles, most of which were rejected online. Of the remaining rate, we studied the single-site  $\gamma$ -ray events and compared them with the rate expected from Monte Carlo simulations of the known atmospheric and cosmic diffuse background. We find a good agreement between data and expectation. This result is very encouraging for the LXeTPC detector technology for the field of MeV  $\gamma$ -ray astronomy.

## ACKNOWLEDGMENTS

We would like to thank Chun Zhang for his contribution in the preparation of the balloon flight in year 2000. This work was supported by NASA under grant NAG5-5108.

## REFERENCES

1. Aprile E., et al., 1998, NIM A 412, 425
2. Aprile E., et al., 2001, NIM A 461, 256-261
3. Aprile E., et al., in: Vol. 4140 of Proc. of SPIE, 2000, pp. 344–359, astro-ph/0012297.
4. Aprile E., et al., 2000, in: M. L. McConnell, J. M. Ryan (Eds.), Vol. 510 of AIP Conf. Proc., AIP, New York, 2000, pp. 799–803.
5. Aprile E., et al., in: Vol. 4140 of Proc. of SPIE, 2000, pp. 333–343, astro-ph/0012398.
6. Aprile E., et al., 2001, IEEE Trans. Nucl. Sci., Vol. 48, NO. 4, pp. 1299–1305, astro-ph/0012276.
7. Oberlack U., et al., 2001, IEEE Trans. Nucl. Sci., Vol. 48, NO. 4, pp. 1041–1047, astro-ph/0012395.
8. Oberlack U., et al., in: Vol. 4141 of Proc. of SPIE, 2000, pp. 168–177, astro-ph/0012296.

9. GEANT, Detector Description and Simulation Tools, CERN Program Library, Long Writeup W5013
10. GCALOR: <http://www.physik.uni-mainz.de/zeitnitz/gcalor/gcalor.html>
11. Schönfelder V., et al., 1980, ApJ 240, 350
12. Kappadath S. C., et al., 1996, AAS 120, 619
13. Costa E., et al., 1984, ApSS 100, 165
14. M.A. Kirsanov, et al., 1993, NIM A 327, 48
15. S.E. Ulin, et al., in: Proc. of SPIE, 42<sup>nd</sup> annual meeting